12-2007

Closed-Form Derivations of ISI and MUI for Time-Reversed Ultra Wideband

K. Popovski
University of Wollongong, keni@uow.edu.au

Beata J. Wysocki
University of Nebraska-Lincoln, bwysocki2@unl.edu

Tadeusz Wysocki
University of Nebraska-Lincoln, wysocki@uow.edu.au

Closed-Form Derivations of ISI and MUI for Time-Reversed Ultra Wideband

K. Popovski, *Member, IEEE,* T. A. Wysocki, *Senior Member, IEEE,* and B. J. Wysocki
School of Electrical, Computer and Telecommunications Engineering
University of Wollongong, Northfields Ave, Wollongong, NSW, 2522, Australia
Email: {keni, wysocki, bjw}@uow.edu.au

***Abstract*—Through transmitter pre-filtering, a time reversed UWB system is capable if harnessing a multipath channel to achieve temporal and spatial focusing. Unfortunately, large RMS channel delay spread leads to significant intersymbol and multi-user interference. This paper presents closed-form expressions for self and multi-user interference for a UWB system utilizing a time-reversed approach. The influence of user multiplexing codes is taken to account through incorporation of a 'separation probability', which characterizes a family of hopping sequences. The standardized IEEE 802.15.3a channel model is applied, and the derived performances are compared with that of a simulated time hopped time-reversed UWB system.**

***Index Terms*—UWB, time-reversed, pre-rake equalization, time hopping, inter-symbol interference, multi-user interference**

I. Introduction

ULTRA Wideband (UWB), or impulse radio, has seen significant attention since its release for commercial applications in early 2002 [1]. It is characterized by having a fractional bandwidth of more than 20%, or bandwidth occupancy greater than 500 MHz [2].

This paper is focused on an extension to time hopped UWB (TH-UWB) [3]. Within TH-UWB, pulses transmitted are either delayed in time (pulse position modulation (PPM)) or changed in amplitude (pulse amplitude modulation (PAM)) for encoding data. Users are multiplexed through code division multiple access based upon a family of orthogonal time hopping codes.

The aforementioned 'extension' is a channel equalization scheme herein referred to as the 'time reversed' (TR) approach, which has its origins in underwater acoustics [4]. While a conventional system would operate with the transmission of sub-nanosecond width Gaussian waveforms, a TR-UWB system uses the channel impulse response from the transmitter to the receiver as a transmit pre-filter. With the channel being estimated through the use of a pilot test signal, a time reversed signal focuses both in time (temporal focusing) and in space (spatial focusing) at the intended receiver, resulting in an autocorrelation of the response being received [5].

The overlap of transmissions for consecutive symbols leads to the effect of inter-pulse, inter-frame, and inter-symbol interference, herein collectively referred to as inter-symbol interference (ISI). Multi-user interference presents a more severe degradation than ISI, with large delay spreads of transmissions causing interference by other transmitters in close proximity.

Consideration for hopping sequences is generally conducted through partial cross correlation equations [6] or traditional Hamming correlations [7]. This paper presents a unique approach to the sequence based performance analysis, developing a set of state probabilities for pulse separations within a TR-UWB system, specific to a family of hopping codes. Derivations presented are based upon core interference equations introduced in [8], adopting similar channel and system parameters.

This paper is organized as follows: Section II outlines a TR-UWB system, together with the channel model and BER calculation method applied; Section III overviews the time hopping code analysis used to account for a multi-user system, together with closed-form solutions for the ISI and MUI present in downlink UWB communications; and Section IV compares the performance of derived formulas to simulated results. Finally, Section V gives all concluding statements and remarks.

II. System Description

A. Signal Equations

The signal $s^{(u)}(t)$ transmitted for the uth user in a time-hopped time-reversed UWB system, with equiprobable data $b_m^{(u)} \in \{-1, 1\}$ mapped through binary PPM with the time shift ε set to equal the pulse width, is given by [9]:

$$s^{(u)}(t) = \frac{\sqrt{E_{TX}(u)}}{\sqrt{G_{H,u;x}}}\left(\sum_{m=-\infty}^{\infty} w\Big(t - mT_f - c_m^{(u)}T_c - \varepsilon b_m^{(u)}\Big)\right) \otimes h(u; x, -t), \tag{1}$$

where $E_{TX}(u)$ is the user signal energy, $w(t)$ is the base transmitted waveform of width T_w seconds, m is the frame number, $G_{H,u;x}$ represents the gain of the channel required for normalization, and x is the position of the receiver. T_f is a single frame length, which is segmented into equally spaced intervals called 'chips' of duration T_c, such that $T_f = N_h T_c$. $c_m^{(u)}$ denotes the position within the particular frame (the chip number) that is occupied by the uth user's signal in accordance with a time hopping sequence. It should be noted that a perfectly power controlled system is assumed, whereby E_{TX} is constant for all users. For the purpose of this paper the pulse shape was set as the second derivative of the Gaussian pulse, with center frequency f_0, defined as [10]:

$$w(t) = \left[1 - 2(\pi t f_0)^2\right] \exp\left\{-(\pi t f_0)^2\right\}, \tag{2}$$

with energy normalized Fourier transform of:

$$\widetilde{W}(f) = \sqrt{\frac{\sqrt{32\pi \cdot f_o^2}}{3}} \frac{2}{\sqrt{\pi \cdot f_o^2}} \left(\frac{f}{f_0}\right)^2 \exp\left\{-\frac{f^2}{f_0^2}\right\}. \quad (3)$$

A center frequency of 3.9GHz was used, which results in a monocycle width of T_w = 0.5ns.

If two users simultaneously occupy the same chip, a collision or 'hit' occurs. The characterizing parameters of these time hopping codes are the cardinality (N_h), which specifies the alphabet size; and the periodicity (N_p), which indicates the length of the code before it is repeated.

Defining the data rate as R, and the number of transmissions per symbol N_s, the frame and chip durations can be represented as $T_f = 1/(N_s R)$ and $T_c = 1/(N_h N_s R)$ respectively.

The signal received is given as:

$$r(t) = \left(\sum_{u=1}^{N_u} s^{(u)}(t) \otimes h(u;x,t)\right) + n(t). \quad (4)$$

A summation takes to account contributions of all N_u users. It should be noted that all transmitters were assumed dispersed enough such that the channel responses from each N_u transmitter to any receiver are independent. As such, each convolution is calculated using the response from user u to the desired receiver. Additive white Gaussian noise with variance of $N_0/2$ is also present.

The decision variable is constructed as an inner product of the received signal (which includes all ISI and MUI degradations) with the receiver template $g(t) = w(t) - w(t-\varepsilon)$, giving the estimated received data of $\hat{b}_m^{(u)}$. The $(L-1)$th path, which has the largest peak in the received signal, is the in-phase autocorrelation peak position for the channel response. This peak has a magnitude related to the number of paths present within the channel. The template for free-space propagation was applied in order to characterize a system which is performance-equivalent to a UWB system employing an All-RAKE receiver.

The multipath model applied is the IEEE 802.15.3a channel, based on the SV model where multipath components arrive in clusters [11]. For the purpose of simulation and closed-form derivations, the discrete-time channel impulse response is modeled as:

$$h(u;x,t) = X \sum_{k=0}^{L-1} \alpha_k \delta(t - \tau_k), \quad (5)$$

where α_k is the path magnitude, τ_k is the time shift, $\delta(t)$ the Dirac delta function, and shadowing is represented by the log-normal term X. The model constitutes a segmentation of path into 'bins' of time width τ (where $\tau_k = \tau \cdot k$), forming a total of L paths, each representing the energy within the bin width. Thus the total channel width is equivalent to $L\tau$. The gain of the α_k coefficients is normalized to unity for each channel realization, and total multipath gain $G_{H,u;x} = \sqrt{X}$. A quasi-stationary channel is assumed, remaining time-invariant for the transmission of a block of data, and independent between blocks.

For the development of closed-form expressions for ISI and MUI, defining $\beta_k = \alpha_{(L-1)-k}$, the discrete time reversed channel response is represented as:

$$h(u;x,-t) = X \sum_{k=0}^{L-1} \beta_k \delta\left(t - \left(L\tau - \tau_{(L-1)-k}\right)\right). \quad (6)$$

B. Error Performance

For a binary PPM UWB system sending N_s transmissions per symbol, the error probability curve is defined as [12]:

$$\mathrm{Pr_e} = Q\left(\sqrt{N_s \cdot \mathit{SINR}}\right) \Rightarrow \frac{1}{2} erfc\left(\sqrt{\frac{N_s \cdot \mathit{SINR}}{2}}\right), \quad (7)$$

where *SINR* represents the signal to combined noise, ISI and MUI ratio. In order for this equation to hold, it must be true that all parameters of the *SINR* are Gaussian distributed. The additive white noise exhibited by the system is defined as a statistically independent zero mean Gaussian random variable [12]. The ISI and MUI terms may be brought under the standard Gaussian approximation provided that the number of paths within the channel impulse responses, the number of users (for MUI), the number of transmissions per symbol, and the bit rate are large enough [13].

Although the received signal power, represented as $P_{RX}(u)$, may arrive at the receiver, only the power in the main autocorrelation peak is used for decoding data ($(L-1)$th path). This is accounted for by an additional ratio ϕ, which represents the ratio of power within the strongest path to the remaining sidelobe power. It was obtained by taking an average over 1000 random instances of a UWB channel. The final *SINR* is:

$$\mathit{SINR} = \frac{\phi \cdot P_{RX}(u)}{\sigma_{AWGN}^2 + \sigma_{ISI}^2 + \sigma_{MUI}^2}. \quad (8)$$

III. Equation Derivations

A. Time Hopping Code Analysis

Assuming a perfectly power controlled system, where users are transmitting at identical data rates, the distinguishing factor for user performance is the time hopping code that is used. Derivations in this paper are based upon a chip separation probability S_e. ISI is controlled by the separation between consecutive elements within a time hopping sequence, while MUI is affected by the relative separation between symbols sent from the interfering users, and those from the desired user.

The chip separation probability $S_e(A,B)$ defines a set of state probabilities which indicate the probability of two transmissions having a certain separation, based upon a family of time hopping sequences. It is determined for a certain separation B between elements of a hopping sequence, and a number A of intermediate pulses transmitted by the user over those B chips. The issue of intermediate pulses over the separation distance is important since the RMS delay spread of a signal may cause interference from a single transmission to last well over an adjacent frame. However, similarity between the separations for varying A allows $S_e(A,B)$ to be approximated by $S_e(0,B)$ for all A. For ISI, S_e was determined for

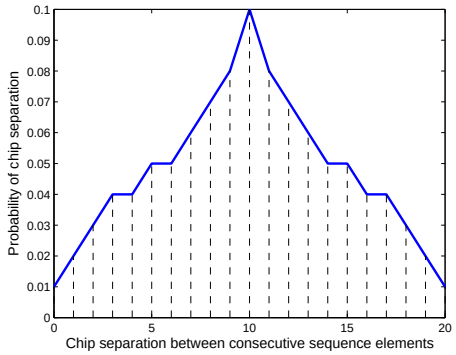

Fig. 1. ISI chip separation probabilities for Reed-Solomon codes

individual hopping codes within a family of sequences, then averaged; while for MUI the analysis was conducted over all possible sequence pairs. The separation B ranges from AN_h to $(A+2)N_h - 2$.

This paper focuses on Reed-Solomon time hopping codes [14]. The ISI chip separation probabilities for this sequence family for a cardinality of $N_h = 11$, no intermediary pulses ($A = 0$), and separation ranging from 0 to $2N_h - 2$ is given in Fig. 1. These probabilities were determined through a brute force analysis of all codes within a given family of sequences, and then averaged for each B.

B. Closed-Form ISI Variance

Intersymbol interference occurs in communications due to an overlap of transmissions as seen at the receiver side. The following derivation of a closed-form representation of ISI within a TR-UWB system is based upon Eq. (16) within [8]. The base expression for inter-symbol interference is:

$$\sigma^2_{ISI} = \sum_{\sigma=1}^{(N_{ov}-1)} \sum_{\varsigma=0}^{2(N_h-1)} (\chi_{\sigma,\varsigma,\xi} + \chi_{\sigma,\varsigma,\psi}), \tag{9}$$

where:

$$\chi_{\sigma,\varsigma,\nu} = S_e\left(\sigma-1,\varsigma\right) \cdot \mathrm{var}\left(h(1;x_1,t) \otimes \left[\sqrt{\frac{E_{TX}(1)}{G_{H,1;x_1}}} \cdot \nu \right] \right),$$

$$\xi = \sum_{k=N_w}^{L-1} \beta_{k+1} w(t - \tau_{k-N_w}),$$

$$\psi = \sum_{k=0}^{N_l-1} \beta_{k+1} w(t - \tau_{k+N_w}),$$

and:

$$N_w = \left\lceil \frac{(\sigma-1)T_f + (\varsigma+1)T_c}{\tau} \right\rceil,$$

$$N_l = L - N_w,$$

$$N_{ov} = \left\lceil \frac{L\tau}{T_f} \right\rceil.$$

Equation (9) relies on a symbol based approach to evaluate the ISI variance. In order to aid in derivations, a shift of the variance position was made, forming the 'time combined' version:

$$\sigma^2_{ISI} = \mathrm{var}\left(\sqrt{\frac{E_{TX}(1)}{G_{H,1;x_1}}} \left\{ \Omega \otimes h(1;x_1,t) \right\} \right), \tag{10}$$

with:

$$\Omega = \sum_{\sigma=1}^{N_{ov}-1} \left\{ \sum_{\varsigma=0}^{2(N_h-1)} S_e(\sigma-1,\varsigma) \left(\sum_{k=0}^{N_l-1} \beta_k w(t-\tau_k) + \sum_{k=N_w}^{L-1} \beta_k w(t-\tau_k) \right) \right\} \tag{11}$$

representing the summation of all interfering partial signals, together with their respective separation probabilities. This was achieved through the a multiplier of $L\tau/T_f$, which is equivalent to the energy normalization required in (9) to adjust for changing data rate and channel delay spread. It should be noted that the multiplier also takes into consideration the movement of the separation probability.

For brevity, as this ISI derivation is concentrated on a single user scenario, user number $u = 1$ and receiver position x_1 are omitted.

Under the assumption that the separation probability is static over σ, the summation over k may be conducted before the summation over σ. Noting the inverse relationship between σ and k through N_l, applying this conversion removes dependence of β_k and α_k terms on σ, yielding:

$$\Omega = \sum_{\varsigma=0}^{2(N_h-1)} S_e(0,\varsigma) \sum_{k=0}^{L-1} \left\{ \left(\beta_k w(t-\tau_k) + \alpha_k w(t-\tau_{L-1-k}) \right) \times \frac{(L-1-k)\tau - (\varsigma+1)T_c}{T_f} \right\}, \tag{12}$$

with, $\lfloor (L\tau - (\varsigma+1)T_c)/\tau \rfloor \approx L-1$. This assumption is valid provided that $N_h \ll L$, as $\max\{\varsigma\}$ is controlled by N_h.

The parameter Ω can be further simplified by considering the summation of both α_k and β_k for all $k \in [0, L-1]$. Summing like terms results in a constant coefficient for all k over α_k, equal to $((L-1)\tau - 2(\varsigma+1)T_c)/T_f$. Hence the ISI formula (10) can be reduced to:

$$\sigma^2_{ISI} = \frac{E_{TX}}{G_H} \cdot S_\Xi \cdot V_{ACF}, \tag{13}$$

where,

$$S_\Xi = \left(\left[\sum_{\varsigma=0}^{2(N_h-1)} S_e\left(0,\varsigma\right) \cdot \frac{(L-1)\tau - 2(\varsigma+1)T_c}{T_f} \right] \right)^2,$$

$$V_{ACF} = \mathrm{var}\left\{ [h(-t) \otimes w(t) \otimes h(t)] \right\},$$

with V_{ACF} defining the variance of the autocorrelation of the channel impulse response convoluted with the base waveform $w(t)$. It can be represented through the use of Fourier transforms, after applying convolutional and autocorrelation properties presented in [12], as:

$$V_{ACF} = \mathrm{var}\left\{ \widetilde{W}(f) \cdot |H(f)|^2 \right\}, \tag{14}$$

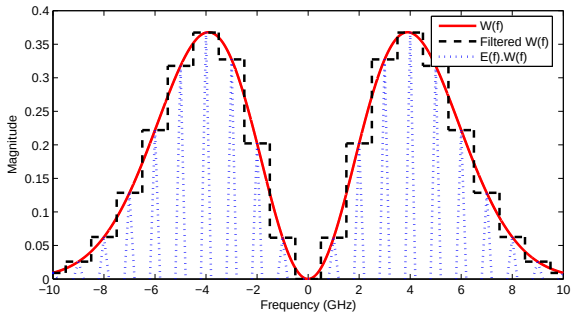

Fig. 2. Zero-order hold filtering of base waveform

where Parseval's Theorem equates the energy over time and frequency domains. Here, $\widetilde{W}(f)$ and $H(f)$ refer to the Fourier transforms of the energy normalized base waveform, as in Eq. (3), and the channel response respectively.

For the purpose of this paper, $h(t)$ was estimated through the use of a single exponential function $e(t)$. Since the discrete version of the channel response is used, this exponential was sampled through the use of the Shah function [15]. Together with a substitution of (3), the autocorrelation variance transforms to:

$$V_{ACF} = \sqrt{\frac{32}{\pi}} \cdot \frac{4}{3 f_o \tau_{bin}^4} \cdot \mathrm{var}\left\{ \left(\frac{f}{f_0}\right)^2 e^{\left(-\frac{f^2}{f_0^2}\right)} \cdot \left| \sum_{i=-\infty}^{\infty} E\left(f - \frac{i}{\tau_{bin}}\right) \right|^2 \right\}. \quad (15)$$

with $E(f)$ representing the Fourier transform of $e(t)$, and the Shah function acting as a replicator of $E(f)$ over the frequency domain.

Under the assumption that $E(f)$ has a bandwidth lower than $1/\tau_{bin}$, which is valid for an exponential $e(t)$, the argument of the variance can be determined by assuming a constant value for the base waveform's frequency response over each $1/\tau_{bin}$ width, as shown in Fig. 2. Here, a zero-order hold filtering has been applied as:

$$\overline{W}(f) = \sum_{i=-\infty}^{\infty} \widetilde{W}\left(\frac{i}{\tau_{bin}}\right) \cdot \Pi\left(\frac{f - iF_{bin}}{F_{bin}}\right), \quad (16)$$

with F_{bin} as the reciprocal of τ_{bin}, and $\Pi(f)$ the rectangular function. This reduces V_{ACF} to:

$$V_{ACF} = \sqrt{\frac{32}{\pi}} \cdot \frac{4}{3 f_o \tau_{bin}^4} \cdot \sum_{i=-\lceil f_{\max}\tau_{bin}\rceil}^{\lceil f_{\max}\tau_{bin}\rceil} \widetilde{W}\left(\frac{i}{\tau_{bin}}\right)^2 \cdot \sum_f |E(f)|^4 \cdot \frac{1}{T_\nu} \cdot \frac{1}{T_w f_c} \quad (17)$$

where f_{max} is the single side frequency over which the majority of the energy within $\widetilde{W}(f)$ exists. The final two terms are required to determine the power spectral density variance, with $T_\nu \approx (2L\tau_{bin} + T_w)$ representing the time width of the signal V_{ACF}, and the final multiplication normalizes based upon the pulse width and sampling frequency. Thus, the final estimate on the ISI variance of a time-reversed UWB system is defined as:

$$\sigma_{ISI}^2 = \frac{E_{TX}}{G_H} \cdot S_\Xi \cdot \mathrm{K} \cdot \Psi, \quad (18)$$

where,

$$S_\Xi = \left(\left[\sum_{\varsigma=0}^{2(N_h-1)} S_e(0,\varsigma) \cdot \frac{(L-1)\tau - 2(\varsigma+1)T_c}{T_f} \right] \right)^2,$$

$$\mathrm{K} = \sqrt{\frac{32}{\pi}} \cdot \frac{4}{3 f_o \tau_{bin}^4} \cdot \frac{1}{L\tau_{bin}} \cdot \frac{1}{T_w f_c},$$

$$\Psi = \sum_{i=-\lceil f_{\max}\tau_{bin}\rceil}^{\lceil f_{\max}\tau_{bin}\rceil} \widetilde{W}\left(\frac{i}{\tau_{bin}}\right)^2 \cdot \sum_f |E(f)|^4.$$

The final requirement is the calculation of the $4th$ moment of the channel envelope estimation $E(f)$. Although the power distribution of a UWB channel model is more complex, $e(t)$ is taken as a single exponential function for simplification of calculations. Its time and frequency domain expressions are [12]:

$$Ae^{-a|t|} \Leftrightarrow \frac{2Aa}{a^2 + 4\pi^2 f^2}. \quad (19)$$

C. Closed-Form MUI Variance

1) In-Phase MUI: In-Phase MUI encompasses the portion of interference from users in close proximity that occurs within the same time frame as the transmission from the desired user. The main technique to combat this form of degradation is the use of time hopping codes employed to arrange users such that minimal same-frame interference is caused.

The In-Phase component covers MUI over the $2N_h - 1$ possible chip separations between the desired and interfering user transmissions. Derivation of its variance requires the application of the MUI sequence analysis outlined in Section III-A.

The derivation presented next is based upon Eq. (17) within [8]. The base expression for the In-Phase MUI from a single user is:

$$\sigma_{InPhaseMUI}^2 = \sum_{\Phi=-(N_h-1)}^{0} \chi_{\Phi,\xi} + \sum_{\Phi=1}^{N_h-1} \chi_{\Phi,\psi}, \quad (20)$$

where:

$$\chi_{\Phi,\nu} = Se(0, \Phi + (N_h - 1) + 1) \cdot \mathrm{var}\left(h(u; x_1, t) \otimes \left[\sqrt{\frac{E_{TX}(u)}{G_{H,u;x_1}}} \cdot \nu \right] \right),$$

$$\xi = \sum_{k=N_{w(In)}}^{L-1} \beta_{k+1} w(t - \tau_{k-N_{w(In)}}),$$

$$\psi = \sum_{k=0}^{N_{l(In)}-1} \beta_{k+1} w(t - \tau_{k+N_{w(In)}}),$$

with:

$$N_{w(In)} = \lceil |\Phi| \cdot T_c/\tau \rceil,$$

$$N_{l(In)} = L - N_{w(In)},$$

Equation (20) estimates the variance through the combination of all partial signals ν which could interfere within the same frame as the desired user's symbol, multiplied by their corresponding separation probability.

In order to obtain a simple solution to this expression, it is assumed that the channel delay spread is significantly larger than the maximum separation $(2N_h-1)$, such that each partial signal ν can be assumed by an entire channel response. This approximation becomes more valid as the data rate and N_s values are increased. The variance can thus be written as:

$$\sigma^2_{InPhaseMUI} \approx \sum_{\Phi=-(N_h-1)}^{N_h-1} Se\left(0,\Phi+(N_h-1)+1\right) \cdot\mathrm{var}\left(h(u;x_1,t)\otimes\left[\sqrt{\frac{E_{TX}(u)}{G_{H,u;x_1}}}\cdot v\right]\right). \quad (21)$$

With known channel delay spread ($L\tau$) and gain ($G_{H,u;x_1}$), the convolution with the propagation channel can be omitted. The disadvantage however is that the structure of the channel is not taken into account. Assuming that a correlation of a time reversed signal with a propagation channel (of equal length) doubles the signal vector length, and noting that ν has normalized energy, (21) can be simplified to:

$$\begin{aligned}\sigma^2_{InPhaseMUI} &= E_{TX}(u)\cdot G_{H,u;x_1} \\ &\cdot \sum_{\Phi=-(N_h-1)}^{N_h-1} Se\left(0,\Phi+(N_h-1)+1\right)\cdot f_c/(L\tau f_c-1)/2 \\ &\approx \frac{E_{TX}(u)\cdot G_{H,u;x_1}}{2L\tau}, \end{aligned} \quad (22)$$

where the sum of all separation probabilities is equal to unit probability. Note the final result requires a multiplication by the number of interfering users.

2) Out-Phase MUI: Out-Phase MUI considers interference caused by nearby users which originate from frames adjacent to the current frame of the desired user. With the high data rates required by emerging UWB applications, this form of interference poses a higher severity than In-Phase MUI.

The variance of this degradation is calculated by summing all partial transmissions which overlap into the desired user's symbol. This summation is conducted over all overlapping time frames (σ), also over all possible separations (ς) between the interfering signal and desired signal, taking into consideration the separation probability. The expression for the Out-Phase MUI by a single user is given by Eq. (18) in [8] as:

$$\sigma^2_{OutPhaseMUI} = \sum_{\sigma=1}^{(N_{ov}-1)}\sum_{\varsigma=0}^{2(N_h-1)} (\chi_{\sigma,\varsigma,\xi}+\chi_{\sigma,\varsigma,\psi}), \quad (23)$$

where:

$$\chi_{\sigma,\varsigma,\nu} = S_e\left(0,\varsigma\right)\cdot\mathrm{var}\left(h(u;x_1,t)\otimes\left[\sqrt{\tfrac{E_{TX}(u)}{G_{H,u;x_1}}}\cdot\nu\right]\right),$$

$$\xi = \sum_{k=N_{w(Out)}}^{L-1}\beta_{k+1}w(t-\tau_{k-N_{w(Out)}}),$$

$$\psi = \sum_{k=0}^{N_{l(Out)}-1}\beta_{k+1}w(t-\tau_{k+N_{w(Out)}}),$$

$$N_{w(Out)} = \left\lceil\frac{(\sigma-1)T_f+(\varsigma+1)\,T_c}{\tau}\right\rceil,$$

$$N_{l(Out)} = L-N_{w(Out)},$$

The similarity between the Out-Phase MUI and ISI equations is evident, although here the user number $u \neq 1$. An alternate approach to the ISI derivation was applied for the Out-Phase MUI however, calculating the variance of the overlapping signals.

The initial simplification is the assumption that interference that originates from frames before the current transmission and that which will interfere in subsequent frames are independent. Also, as in In-Phase MUI, the convolution has been removed, which once again requires a division by 2 due to the halving of the output length. For brevity, constant energy/gain multiplications have been omitted, assuming normalized channels. Neglecting the time shifting on τ, as variance is independent of time position, and using the relationship that $\beta_k = \alpha_{(L-1)-k}$, (23) simplifies to:

$$\sigma^2_{OutPhaseMUI} = \frac{1}{2}\sum_{\varsigma=0}^{2(N_h-1)} S_e\left(0,\varsigma\right)\Upsilon, \quad (24)$$

where:

$$\Upsilon = \sum_{\sigma=1}^{N_{ov}-1}\left(\mathrm{var}\left(\sum_{k=0}^{N_{l(Out)}-1}\left[\beta_{k+1}w(t-\tau_k)+\alpha_{k+1}w(t-\tau_{L-1-k})\right]\right)\right).$$

Encompassing the summation over σ into the variance is not feasible due to correlation of the signals existing in different frames. In order to remove this correlation, an additional time shift of twice the channel delay spread may be introduced, otherwise the correlation between the variables within the *var* function must be considered. Taking the summation over k to produce a single independent signal, correlation exists for the $N_{ov}-1$ signals, herein referred to as v_σ, when summed over σ. This is accounted for by subtracting twice the covariance between all $N_{ov}-1$ signals, defined as Θ. Expressing (24) as:

$$\sigma^2_{OutPhaseMUI} = \frac{1}{2}\sum_{\varsigma=0}^{2(N_h-1)} S_e\left(0,\varsigma\right)\cdot N_{ov}\cdot\mathrm{var}\left(\sum_{\sigma=1}^{N_{ov}-1} v_\sigma\right), \quad (25)$$

the covariance between the dependent signals is:

$$\Theta = \sum_{\sigma_1=1}^{N_{ov}-1}\sum_{\substack{\sigma_2=1\\ \sigma_2\neq\sigma_1}}^{N_{ov}-1}\mathrm{cov}[\nu_{\sigma_1},\nu_{\sigma_2}]. \quad (26)$$

Conceptually, it can be seen that the $N_{ov}-1$ signals being correlated are replicas of the time reversed channel impulse response, with portions attenuated or nulled. For example, at $N_{l(Out)} = L/2$, the summation over k magnifies β_k from τ_0 to $\tau_{L/2-1}$, and α_k values from τ_{L-1} to $\tau_{L/2-1}$. Together these form the complete time reversed response. Through examination of the covariance of the partial signals, it was determined that Θ is equal to the summation of the signal energy of all partial responses with $N_{l(Out)} < L/2$, together with the variance of the entire channel multiplied by a factor θ_{hf}. Assuming the channel is zero mean, this variance reduces

to the calculation of the gain of the normalized channel, which by definition is unity. Hence Θ may be expressed as:

$$\Theta = \frac{1}{2L\tau}\left\{\left[\sum_{\xi=\lfloor N_{ov}/2\rfloor+1}^{N_{ov}-1}\sum_{l=0}^{N_l-1}\left(\alpha_{l+1}^2+\beta_{l+1}^2\right)\right]+\theta_{hf}\right\}, \tag{27}$$

$$\theta_{hf} = \begin{cases} (N_{ov}-2)+4\sum_{j=1}^{N_{ov}/2-2}(N_{ov}/2-j-1),\ N_{ov}\text{ even} \\ 4\sum_{j=1}^{\lceil N_{ov}/2\rceil-2}\left(\lceil N_{ov}/2\rceil-j-1\right),\ N_{ov}\text{ odd} \end{cases}$$

Here, Θ was estimated based only upon the interference at $\varsigma = N_h - 1$, as this is the median level of interference that the system will face over the $2N_h - 1$ possible chip separations. Also, the normalized base waveform was omitted for simplification, rather focusing on the summation of path gains and accounting for the change in signal lengths through the $2L\tau$ division.

The order of summation over σ and k can now be exchanged as in the ISI derivation, giving:

$$\sigma^2_{OutPhaseMUI} = \frac{1}{2}\sum_{\varsigma=0}^{2(N_h-1)} S_e(0,\varsigma)\cdot\mathrm{var}\left(\sum_{k=0}^{L-1}\sum_{\sigma=1}^{\frac{((L-1)-k)\tau-(\varsigma+1)T_c}{T_f}+1}\left[\beta_{k+1}w(t-\tau_k)+\alpha_{k+1}w(t-\tau_{L-1-k})\right]\right)-2\Theta. \tag{28}$$

As the α_k and β_k terms are independent of σ, the expression can be simplified to obtain a constant multiplier of $\lceil([(L-1)-k]\,\tau-[\varsigma+1]\,T_c)/T_f\rceil$ over all k.

Similar to the ISI derivation, (28) can be reduced by observing that the summation over k adds two instance of each α_k value, each with a multiplier taking the value of either $([L-1-k]\,\tau-[\varsigma+1]\,T_c)/T_f+1/2$ or that of $(k\tau-[\varsigma+1]\,T_c)/T_f+1/2$, where it is assumed that the *ceil* operation will on average add $1/2$ to the fraction. The summation of these weights results in a constant multiplier over k, giving the final expression:

$$\sigma^2_{OutPhaseMUI} = G\cdot E_{TX}\left(\frac{1}{2}\left\{\sum_{\varsigma=0}^{2(N_h-1)} S_e(0,\varsigma)\cdot\left[\frac{(L-1)\tau-2(\varsigma+1)T_c}{T_f}+1\right]^2\right\}\mathrm{var}\left(h(t)\right)-2\Theta\right), \tag{29}$$

where convolution with the energy normalized independent base waveform $w(t)$ has been ignored.

In order to remove all dependence on individual path magnitudes (α_k,β_k), it is observed that the covariance summation Θ in (27) consists of a summation of all channel path amplitudes. Paths closer to $l=\{0,L-1\}$ are summed more times than those at $l=L/2$. Analysis shows that the double summation within Θ results in the square of all path amplitudes multiplied by an envelope which consists of $2(\lceil N_{ov}/2\rceil-1)$ discontinuities, with N_{ov} increments of step width T_f/τ paths. It can be described mathematically as:

$$\widetilde{\Theta}(t) = \sum_{i=1}^{N_{ov}}\Pi\left(\frac{t-T_f/\tau}{T_f/\tau}\right)\cdot\left|\left\lceil\frac{N_{ov}}{2}\right\rceil-i\right|, \tag{30}$$

reducing (27) to:

$$\Theta = \frac{1}{2L\tau}\left\{\left[h^2(t)\widetilde{\Theta}(t)\right]+\theta_{hf}\right\}. \tag{31}$$

As in the ISI derivation, a MMSE exponential estimation was adopted to replicate the structure of the channel response within the Out-Phase MUI. The MMSE estimation of $h(t)$ was used as in Section III-B, with an alternate estimation developed for $h^2(t)$.

It should be noted that the final expression for the multi-user interference from a single interferer ($\sigma^2_{OutPhaseMUI}$) must be multiplied by the total number of interferers: $MUI = MUI_{(\text{Single User})}\cdot(N_u-1)$. Also, and in the ISI derivation, a normalization by $L\tau/T_f$ is required. However this multiplier includes the movement of the separation probability between (9) and (10), which must be compensated here by a multiplication by $1/\sqrt{mean(S_e(0,\varsigma))}$, $\forall\varsigma$.

IV. Comparison of Simulated and Estimated Results

A TR-UWB simulation was adapted from a time hopped PPM UWB simulation by Di Benedetto and Giancola [16]. CM1 in the IEEE 802.15.3a model was tested, which requires a ratio of $\phi\approx 0.566$ for Eq. (8). The cardinality and periodicity of each time hopping code were set to 11, with a pulse width of $0.5ns$, and a data encoding shift of $0.5ns$. The bin width τ was set to $1ns$ and transmit power to $1mW$. The parameters for the exponential estimation of (19) were calculated as $A=0.2858$, $a=7.1\times10^7$ for $h(t)$, and $A=0.122$, $a=1.3\times10^8$ for $h^2(t)$.

Comparative results for the ISI derivation of Section III-B, using Reed-Solomon time hopping, for simulation ('Sim') and variance derivation ('Equ') are shown in Fig. 3(a) and Fig. 3(b), for an N_s of 5 and 10 respectively. Tests were conducted for data rates of 15, 50 and $100Mbit/s$. It can be observed that for all data rates tested, the derived error curve closely traces the simulated performance. As expected, an increase in the data rate, which has a proportional decrease in the frame width T_f, significantly degrades the performance.

Alignment between the formulated MUI performance of Section III-C and simulated results was also evident. Applying Reed-Solomon coding, tests were run for a 10 user scenario at $15Mbit/s$, $N_s=10$, and $30Mbit/s$, $N_s=10$, shown in Fig. 4(a). Performance analysis for a system supporting 5 users was also tested, shown in Fig. 4(b), at a data rate of $30Mbit/s$ and $N_s=5$. All plots reflect the 'maximum', 'minimum', and 'average' performance of the simulated system, together with the formulated performance curve.

In both the ISI and MUI scenarios, an over-approximation develops for the formulated performance as the level of interference increases. This results due to approximations made in the derivation process, although the estimated curve always remains within close proximity to simulated results, generally within a decade of the simulated performance.

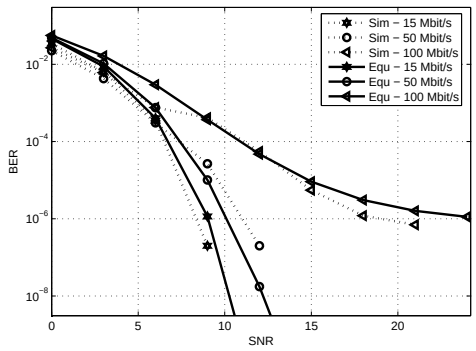

(a)

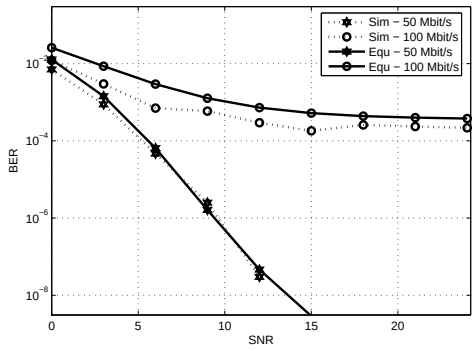

(b)

Fig. 3. ISI BER curves with Reed-Solomon coding for (a) $N_s = 5$ (b) $N_s = 10$

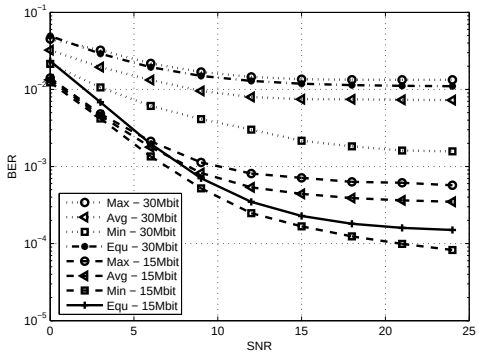

(a)

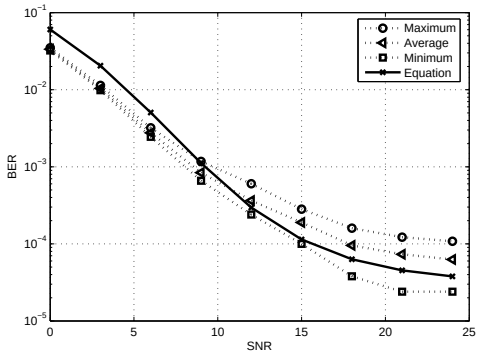

(b)

Fig. 4. MUI BER curves with Reed-Solomon coding for (a) 10 users at $30Mbit/s$, $N_s = 10$ and $15Mbit/s$, $N_s = 10$ (b) 5 users at $30Mbit$, $N_s = 5$

V. Conclusion

In this paper, we have developed closed-form expressions for the ISI and MUI within a time-reversed UWB system. A 'separation probability' parameter was applied for user multiplexing. Comparative results indicate a close alignment between simulated and derived error performance. A slight over-approximation is apparent due to simplification measures applied, although always remaining within close estimation.

Future work that can be conducted in this field includes studying the effects of non-perfect power controlled systems on multi-access performance in a time-reversed UWB architecture.

References

[1] FCC, "New public safety applications and broadband internet access among uses envisioned by fcc authorization of ultra-wideband technology," Unofficial announcement of Commission action, February 2002.

[2] ——, "Revision of part 15 of the commissions rules regarding ultra-wideband transmission systems," Document 00-163, ET Docket No. 98-153, April 2002.

[3] M. Z. Win and R. A. Scholtz, "Impulse radio: How it works," in *IEEE Communications Letters*, vol. 2, no. 2. IEEE, Feb 1998, pp. 36–38.

[4] G. F. Edelmann, T. Akal, W. S. Hodgkiss, S. Kim, W. A. Kuperman, and H. C. Song, "An initial demonstration of underwater acoustic communication using time reversal," *IEEE Journal of Oceanic Engineering*, vol. 27, no. 3, pp. 602–609, July 2002.

[5] T. Strohmer, M. Emami, J. Hansen, G. Papanicolaou, and A. J. Paulraj, "Application of time-reversal with mmse equalizer to uwb communications," in *Global Telecommunications Conference*, vol. 5, November 2004, pp. 3123–3127.

[6] B. Hu and N. C. Beaulieu, "Accurate performance evaluation of time-hopping and direct-sequence uwb systems in multi-user interference," *IEEE Transactions on Communications*, vol. 53, no. 6, pp. 1053–1062, June 2005.

[7] I. Guvenc and H. Arslan, "Design and performance analysis of th sequences for uwb-ir systems," in *Wireless Communications and Networking Conference*, vol. 2, March 2004, pp. 914–919.

[8] K. Popovski, B. J. Wysocki, and T. A. Wysocki, "Modelling and comparative performance analysis of a time reversed uwb system," in *to appear in EURASIP Journal on Wireless Communications and Networking*, 2007.

[9] T. Erseghe, "Time-hopping patterns derived from permutation sequences for ultra-wide-band impulse-radio applications," in *University di Padova*, 2002. [Online]. Available: http://primo.ismb.it/firb/docs/uwb-wseas02.pdf

[10] A. Swami, B. Sadler, and J. Turner, "On the coexistence of ultra-wideband and narrowband radio systems," in *Military Communications Conference, Communications for Network-Centric Operations: Creating the Information Force*, vol. 1, October 2001, pp. 16–19.

[11] A. Saleh and R. Valenzuela, "A statistical model for indoor multipath propagation," *IEEE Journal on Selected Areas in Communications*, vol. 5, no. 2, pp. 128–137, February 1987.

[12] J. G. Proakis and M. Salehi, *Communication Systems Engineering*, 2nd ed. Prentice Hall, New Jersey, USA, 2002.

[13] M. G. D. Benedetto, "Mac for uwb," 2002, networking with UWB Seminar - UWB Group at University of Rome. [Online]. Available: http://www.icsl.ucla.edu/ spapl/seminar/uwb2.pdf

[14] R. M. Mersereau and T. S. Seay, "Multiple access frequency hopping patterns with low ambiguity," *IEEE Transactions on Aerospace and Electronic Systems*, vol. 17, no. 4, pp. 571–578, July 1981.

[15] E. W. Weisstein, "Shah function," MathWorld. [Online]. Available: http://mathworld.wolfram.com/ShahFunction.html

[16] M.-. G. D. Benedetto and G. Giancola, *Understanding Ultra Wide Band - Radio Fundamentals*. Prentice Hall, 2004.